



Phenomenological Nuclear Potential Shapes for Optical Model Analyses of $^{16}\text{O}+^{12}\text{C}$ Elastic Scattering

Gökhan COF¹, Mehmet Ertan KÜRKCÜOĞLU*²

¹ Süleyman Demirel University, Graduate School of Natural and Applied Sciences, 32260, Isparta, Turkey

² Süleyman Demirel University, Faculty of Arts and Sciences, Department of Physics, 32260, Isparta, Turkey

*Corresponding author e-mail: ertankurkuoglu@sdu.edu.tr

(Alınış / Received: 03.10.2019, Kabul / Accepted: 11.11.2019, Yayınlanma / Published: 30.11.2019)

Abstract: Optical model analyses of the $^{16}\text{O}+^{12}\text{C}$ elastic scattering at the incident energies $E_{LAB}=62, 75, 80, 94.8, 100, 115.9$ and 124 MeV were performed by using different phenomenological potential forms. Possible complex nuclear potential forms, which would provide a certain degree of agreement between the experimental data and the theoretical calculations, were examined in the construction of the optical potential. The structure of the considered nuclear potentials consisted of a deep, attractive, WS2 (Woods-Saxon square) type real part and relatively shallow, absorptive imaginary parts. The imaginary potential shapes investigated in this study were chosen in four different forms; WS_V (Woods-Saxon volume), WS2_V , WS_V+WSD_S (Woods-Saxon Differential surface) and $\text{WS2}_V+\text{WSD}_S$. It was found that, the analyses with the potentials having WS_V+WSD_S type and $\text{WS2}_V+\text{WSD}_S$ type imaginary parts produced similar results that explained the differential cross-section measurements of the $^{16}\text{O}+^{12}\text{C}$ system better than the other phenomenological potential forms. The agreement between the theoretical analyses and the experimental data was determined by using usual χ^2 criterion.

Key words: Elastic scattering, Optical model, Cross-section

$^{16}\text{O}+^{12}\text{C}$ Esnek Saçılmasının Optik Model Analizleri için Fenomenolojik Nükleer Potansiyel Şekilleri

Özet: $^{16}\text{O}+^{12}\text{C}$ esnek saçılmasının optik model analizleri, farklı fenomenolojik potansiyel formları kullanılarak $E_{LAB}=62, 75, 80, 94.8, 100, 115.9$ ve 124 MeV gelme enerjileri için çalışıldı. Optik potansiyelin inşasında, deneysel veriler ile teorik hesaplamalar arasında belirli bir düzeyde uyum sağlanmasına imkân verebilecek karmaşık nükleer potansiyel formları denendi. İlgili nükleer potansiyellerin yapısı; derin, çekici, WS2 (Woods-Saxon kare) formunda gerçel bir kısım ile nispeten sığ, soğurucu sanal kısımlardan oluşturuldu. Bu çalışmada araştırılan sanal potansiyeller; WS_H (Woods-Saxon hacim), WS2_H , WS_H+WSD_Y (Woods-Saxon Diferansiyel yüzey) ve $\text{WS2}_H+\text{WSD}_Y$ olmak üzere 4 farklı formda seçildi. WS_H+WSD_Y tipi ve $\text{WS2}_H+\text{WSD}_Y$ tipindeki sanal potansiyeller kullanılarak yapılan analizlerin benzer sonuçlar ürettiği ve $^{16}\text{O}+^{12}\text{C}$ sistemine ait tesir-kesiti ölçümlerini açıklamada, diğer fenomenolojik potansiyel formlarına göre daha başarılı olduğu bulundu. Teorik analizler ile deneysel veriler arasındaki uyum χ^2 hata hesabı ile belirlendi.

Anahtar kelimeler: Elastik saçılma, Optik model, Tesir-kesiti

1. Introduction

The subject concerning the elastic and inelastic interactions of light heavy-ions is an intensively studied topic in nuclear physics. According to the investigations carried out for various scattering experiments, many interesting features about nuclear structure and reactions were revealed.

The explanation of the nuclear interaction mechanism for a reaction requires the solution of many-body problem, which has some exhaustive mathematical difficulties. In the study of nuclear reactions, instead of seeking the solution of the many-body problem between the nucleons of a target and a projectile, the interactions between two nucleon groups can be studied by using simplified models such as the optical model (OM) [1-4], the distorted-wave Born approximation [2, 3] and folding model [1, 2]. In these studies, which based on dynamical models or phenomenological approaches, there are still some problems remaining to explain the nuclear interactions: (i) anomalous large angle scattering, (ii) the phase abnormality between experimental results and theoretical predictions, (iii) producing of the oscillatory structure around the Coulomb barrier, (iv) simultaneous fits of the individual angular distributions, resonances and excitation functions, (v) inconsistency in the use of deformation parameter (β), etc. [5]. OM formalism, however, is broadly used for explaining the elastic scattering mechanism of light heavy-ions [1, 6-23]. Determination of the most suitable model potential shape has primary importance to be able to apply this model successfully for analyzing a specific heavy ion (HI) scattering data in terms of empirical parameters used in the nuclear potential. Thus, the model potential must display the same behaviours as the interaction between two interacting particle groups [1-4].

The refractive effects observed in certain HI interactions, where the scattering is sensitive to the central (nuclear) potential inside the strong absorption radii, have been used as a practical tool for understanding the nature of the OM potential. In particular, these effects have been discussed for $^{16}\text{O}+^{16}\text{O}$ [9, 16, 24, 25], $^{12}\text{C}+^{12}\text{C}$ [1, 26-28] and $^{16}\text{O}+^{12}\text{C}$ [6, 7, 10, 15, 18, 28-32] systems in the literature. Eventually, the reported complex nuclear potentials of those scattering reactions have been described as the composition of deep and attractive potentials for the real part plus weaker and absorbing potentials for the imaginary part. Thus, the conventional WS, WS2, WSD shapes or a combination of these forms have been widely used to build the parts of a phenomenological nuclear potential in the standard OM formalism [33-35].

When the elastic scattering process between oxygen and carbon nuclei is concerned, it can be stated that although there is a consensus about the usage of WS2 shape for the real part, the imaginary parts have been chosen in different forms. In a study, where the $^{16}\text{O}+^{12}\text{C}$ elastic scattering was investigated specifically, measurements and an OM analysis using Woods-Saxon type potentials for seven energies between 62, 75, 80, 94.8, 100, 115.9 and 124 MeV have been reported [6]. While a WS+WSD type potential has been chosen for the imaginary part, WS2 form has been used in the construction of the real part of the nuclear potential by keeping the diffusion parameter and the radius of the real potential fixed to 1.4 fm and 4 fm respectively [6]. In another study carried out for $^{16}\text{O}+^{12}\text{C}$ and $^{18}\text{O}+^{12}\text{C}$ reactions for six energies from 80 to 132 MeV, OM analysis for the elastic scattering mechanism has been described by phenomenological potentials. To reproduce the elastic angular distribution data, a WS2 term has been used for the real part of the nuclear potential and two different forms, a WS type pure volume term and sum of WS2 volume plus WSD surface terms, have been proposed for the

imaginary part [7]. However, no such analysis with WS2+WSD type imaginary potential has been performed for 62 and 75 MeV data. It is emphasized in both studies that the addition of a surface potential term to the imaginary part helps to explain the experimental data better [6,7]. Moreover, Gridnev et al. [36] and Ogloblin et al. [10] have studied the $^{16}\text{O}+^{12}\text{C}$ reaction at the energies higher than 132 MeV by using OM potentials with a WS form for the real part and a WS type pure volume term for the imaginary part.

In the present work, the comparative OM analyses for the $^{16}\text{O}+^{12}\text{C}$ elastic scattering at the energies $E_{LAB}=62, 75, 80, 94.8, 100, 115.9$ and 124 MeV have been performed by using different phenomenological potential shapes for the imaginary part of the nuclear potential. In the following, the general structure of OM potential used in this study has been introduced. Then, the results obtained with phenomenological OM potentials for the $^{16}\text{O}+^{12}\text{C}$ elastic scattering differential cross-section data have been presented and discussed.

2. Material and Method

The standard OM is a straightforward and very successful reaction model for explaining the elastic scattering of HI reactions. In this model, elastic scattering can be interpreted in terms of a model potential, which is an effective interaction between two interacting particle groups [1-4]. The elastic scattering mechanism is treated in a general way by taking into account the behavior of the projectile and by considering the absorption effects. This is done by assuming the absorbed particles vanish in the elastic channels. A complex potential form, which is called the optical potential, is used in OM calculations. The real part of the interaction potential is responsible for the elastic scattering and the imaginary part describes the loss of flux (absorption) into non-elastic channels [2, 3]. After the first optical potential, a complex square-well potential, was introduced by Feshbach et al [37], it has been understood that an appropriate shape for the optical potential can be reached by using Woods-Saxson type phenomenological potentials [38]. The general structure of the Woods-Saxson form factor used in OM calculations can be given as,

$$f^n(r, r_i, a_i) = \frac{1}{[1 + \exp(\frac{r-r_i A^{1/3}}{a_i})]^n} \quad (1)$$

where r is the distance between the centers of the interacting nuclei, r_i represents the reduced radius, a_i is known as diffuseness parameter, $A^{1/3} = A_p^{1/3} + A_t^{1/3}$ where A_p and A_t are the mass numbers of projectile and target respectively. In the equation above, $n=1$ is used for obtaining WS form and $n=2$ is used for WS2 form. The behavior of the WS form factor and its derivative are illustrated in Figure 1, and the difference between WS and WS2 form factor is shown in Figure 2.

In one-channel OM formalism, the structure of effective potential can be given as

$$V(r) = V_{Coul}(r) + V_C(r) + V_l(r) \quad (2)$$

The interaction potential, $V(r)$ in Equation 2 is composed of Coulomb potential, central potential and centrifugal potential respectively. The central potential, $V_C(r)$ consists of real and imaginary components ($V_C(r) = V_{CR}(r) + iW_{CI}(r)$).

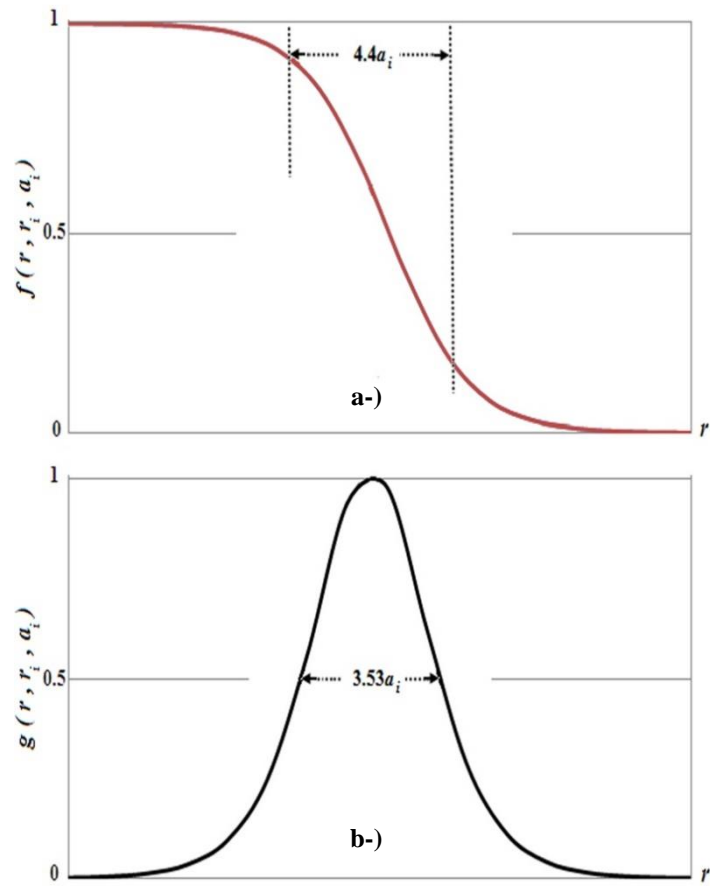


Figure 1. a-) General behavior of the WS form factor function, $f(r, r_i, a_i)$ and b-) its derivative $g(r, r_i, a_i)$. (the form factor, $f(r, r_i, a_i)$ falls from 90% to 10% over a distance $4.4a_i$).

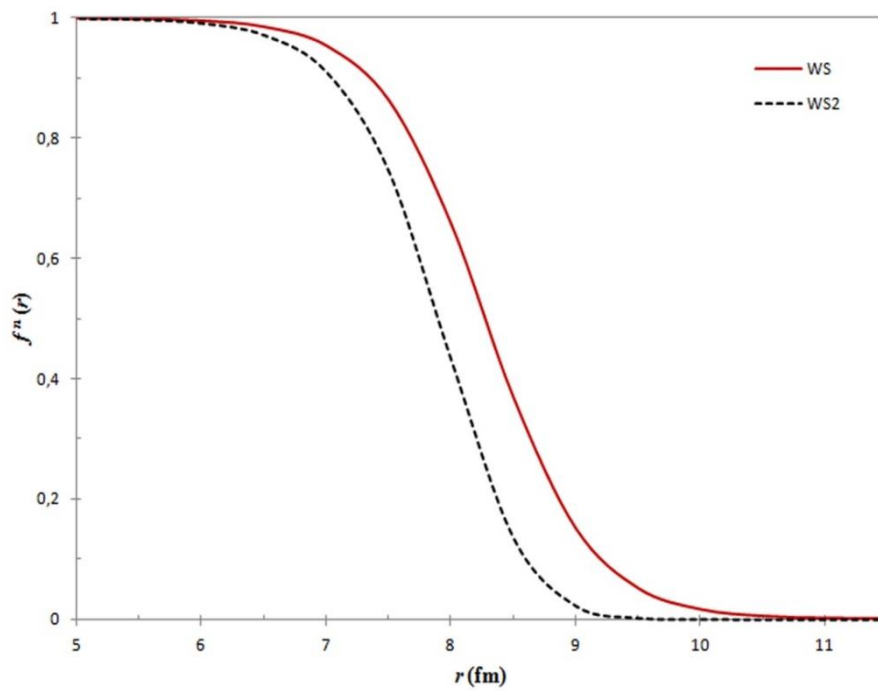


Figure 2. Comparison of WS (red solid line) and WS2 (black dashed line) forms according to the distance r for $^{16}\text{O}+^{12}\text{C}$ system (with the parameters $r_v = 1.72$ fm and $a_v = 0.42$ fm).

Although the Coulomb and centrifugal potentials are well defined, the structure of the central potential is not clear. When studying a HI reaction in OM, the main problem is to find an appropriate central potential shape for better description of the experimental data.

Coulomb potential [2], $V_{Coul}(r)$, which is described as the potential of a uniformly charged sphere with a radius $R_C(r)$ (due to the charge of projectile, $Z_p e$ interacting with the charge of target, $Z_t e$), is represented by

$$V_{Coul}(r) = \begin{cases} \frac{1}{4\pi\epsilon_0} \frac{Z_p Z_t e^2}{r}, & r \geq R_C \\ \frac{1}{4\pi\epsilon_0} \frac{Z_p Z_t e^2}{2R_C} \left(3 - \frac{r^2}{R_C^2}\right), & r < R_C \end{cases} \quad (3)$$

where $R_C = r_c A^{1/3}$ with the Coulomb radius, $r_c = 1.2$ fm [1].

The real part of the central potential, $V_{CR}(r)$ is assumed to have WS2 shape as

$$V_{CR}(r) = \frac{-V_0}{\left[1 + \exp\left(\frac{r - r_0 A^{1/3}}{a_0}\right)\right]^2} \quad (4)$$

The imaginary part of the central potential, $W_{CI}(r)$ is sensitive to the details of the interaction and related to the inelastic scattering process. Although the importance of the imaginary potential becomes more essential in inelastic scattering case, the central potential has to have this imaginary component even for the elastic scattering case.

In the phenomenological OM approach, the imaginary part of the central potential can be represented by either only a pure volume term or by a combination of a volume term plus a surface term as $W_{CI}(r) = V_V(r) + V_S(r)$. The shape of the imaginary volume term is expressed by the equation

$$V_V(r) = \frac{-W_V}{\left[1 + \exp\left(\frac{r - r_V A^{1/3}}{a_V}\right)\right]^n} \quad (5)$$

where the form of this component can be adjusted to WS ($n=1$) or WS2 ($n=2$) shape. The absorption in the nucleus surface can be described by WSD type surface potential as

$$V_S(r) = -4a_S W_S \left\{ -\frac{d}{dr} \left[1 + \exp\left(\frac{r - r_S A^{1/3}}{a_S}\right) \right]^{-1} \right\} \quad (6)$$

In Equations 4-6, the subscripts O , V and S indicate the terms of the real part, imaginary volume and imaginary surface terms respectively for the reduced radii and diffuseness parameters as well as the potential depths V_0 , W_V and W_S .

The centrifugal potential depending on the angular momentum quantum number ℓ , is

$$V_\ell(r) = \frac{\hbar^2 \ell(\ell + 1)}{2\mu r^2}, \quad (7)$$

where μ is the reduced mass of the colliding pair. The reduced mass is given in terms of the mass of the projectile, m_p and the target, m_t by

$$\mu = \frac{m_p m_t}{m_p + m_t}. \quad (8)$$

3. Results

To determine the most suitable interaction potential form for explaining the experimental cross-section data of $^{16}\text{O}+^{12}\text{C}$ elastic scattering [6], OM analyses with different phenomenological nuclear potential sets were studied for $E_{LAB}=62, 75, 80, 94.8, 100, 115.9$ and 124 MeV energies by using the computer code Fresco [39]. The structures of the central potentials examined for this purpose were chosen as follows:

- i-) $V_{C1} = V_{CR}(\text{WS2}) + iW_{CI}(\text{WS}_V)$
- ii-) $V_{C2} = V_{CR}(\text{WS2}) + iW_{CI}(\text{WS2}_V)$
- iii-) $V_{C3} = V_{CR}(\text{WS2}) + iW_{CI}[(\text{WS}_V) + (\text{WSD}_S)]$
- iv-) $V_{C4} = V_{CR}(\text{WS2}) + iW_{CI}[(\text{WS2}_V) + (\text{WSD}_S)]$.

To produce the best fit for the elastic scattering data, whose angular distributions range out to 145 degrees in the center of mass system, we performed our calculations by considering free parameters for the real and imaginary parts. The best parameter values for our analyses are given in Table 1. The results of those four potential sets have been presented in Figure 3. Although all the analyses with present potential sets, in general, exhibited the usual diffraction-like behaviour at the smaller angles (up to around 50 or 60 degrees), V_{C3} and V_{C4} type potential shapes have produced similar results to each other and complied with the data better than the results of V_{C1} and V_{C2} forms. This agrees with the literature that emphasizes the necessity of a surface term in the imaginary part of the central potential [6, 7].

The quality of agreement between the theoretical predictions and experimental angular distribution data has been evaluated by using the usual χ^2 search

$$\chi^2 = \frac{1}{N_\sigma} \sum_{i=1}^{N_\sigma} \frac{(\sigma_{th} - \sigma_{ex})^2}{(\Delta\sigma_{ex})^2}. \quad (9)$$

In this equation, σ_{th} and σ_{ex} are theoretical and experimental cross-sections respectively. $\Delta\sigma_{ex}$ represents the uncertainties in the experimental cross-sections and N_σ shows the total number of the angles measured. A constant experimental error value of 10% has been assigned for the χ^2 calculations at all data points as described in the study of Nicoli et al. [6]. The most appropriate dynamical and geometry parameters of the phenomenological potentials have been defined for our analyses (Table 1) by considering both the lowest χ^2 values and the ability of those parameters to reproduce the phase and period properties of the experimental data. We obtained smaller χ^2 values from the analyses performed with V_{C3} and V_{C4} type central potentials than the outcomes of V_{C1} and V_{C2} type potentials (Table 1).

Table 1. The parameters used in OM analyses of $^{16}\text{O}+^{12}\text{C}$ elastic scattering at 62, 75, 80, 94.8, 100, 115.9 and 124 MeV energies for different phenomenological potential forms, and χ^2 values for these analyses (The shape of the real potential was fixed to WS2 for all the calculations).

Energy (MeV)	Real Part			Imaginary	Imaginary Part						χ^2
	V_0 (MeV)	r_0 (fm)	a_0 (fm)	Potential Shape	W_V (MeV)	r_V (fm)	a_V (fm)	W_S (MeV)	r_S (fm)	a_S (fm)	
62	306.0	0.620	1.790	WS_V	3.98	1.700	0.494	-	-	-	42.7
	317.4	0.593	1.082	WS2_V	12.91	0.905	0.330	-	-	-	88.9
	294.2	0.825	1.350	WS_V+WSD_S	9.61	1.059	0.055	2.55	1.412	0.483	32.7
	305.1	0.821	1.360	WS2_V+WSD_S	16.12	1.045	0.048	2.70	1.361	0.496	34.6
75	307.0	0.631	1.700	WS_V	4.30	1.740	0.470	-	-	-	51.4
	305.0	0.648	1.325	WS2_V	9.80	1.112	0.771	-	-	-	50.8
	282.1	0.835	1.450	WS_V+WSD_S	15.61	1.074	0.092	4.05	1.357	0.333	43.7
	269.5	0.833	1.479	WS2_V+WSD_S	12.69	1.078	0.061	4.23	1.349	0.350	40.3
80	288.6	0.709	2.141	WS_V	5.69	1.723	0.419	-	-	-	54.5
	278.0	0.816	1.326	WS2_V	10.35	1.287	0.414	-	-	-	99.7
	280.5	0.831	1.403	WS_V+WSD_S	12.51	1.028	0.127	2.77	1.364	0.465	32.1
	286.4	0.826	1.400	WS2_V+WSD_S	13.15	1.056	0.150	2.78	1.334	0.459	29.9
94.8	287.0	0.522	1.494	WS_V	05.10	1.620	0.750	-	-	-	59.7
	273.8	0.869	1.273	WS2_V	14.26	1.298	1.267	-	-	-	56.4
	268.4	0.849	1.435	WS_V+WSD_S	13.80	1.072	0.125	03.24	1.369	0.383	34.9
	301.0	0.831	1.401	WS2_V+WSD_S	21.59	0.896	0.038	06.40	1.267	0.371	29.3
100	306.8	0.527	1.724	WS_V	05.51	1.699	0.579	-	-	-	48.7
	284.0	0.637	1.299	WS2_V	13.30	1.093	0.801	-	-	-	38.4
	275.0	0.831	1.405	WS_V+WSD_S	11.90	1.126	0.116	03.24	1.416	0.456	17.3
	282.5	0.838	1.392	WS2_V+WSD_S	10.67	1.103	0.150	04.75	1.329	0.457	17.6
115.9	291.0	0.550	1.369	WS_V	0.814	1.457	0.779	-	-	-	65.9
	237.0	0.388	1.990	WS2_V	20.70	0.924	0.635	-	-	-	61.6
	282.4	0.826	1.416	WS_V+WSD_S	15.10	0.915	0.096	07.00	1.273	0.462	24.4
	282.0	0.836	1.426	WS2_V+WSD_S	16.10	0.925	0.110	07.04	1.269	0.463	23.4
124	297.0	0.420	2.090	WS_V	17.70	1.332	0.463	-	-	-	46.0
	233.0	0.410	1.730	WS2_V	12.50	1.018	0.681	-	-	-	68.6
	316.7	0.841	1.350	WS_V+WSD_S	16.46	1.090	0.099	08.21	1.302	0.406	31.3
	292.7	0.829	1.354	WS2_V+WSD_S	16.16	1.035	0.100	12.11	1.222	0.405	31.3

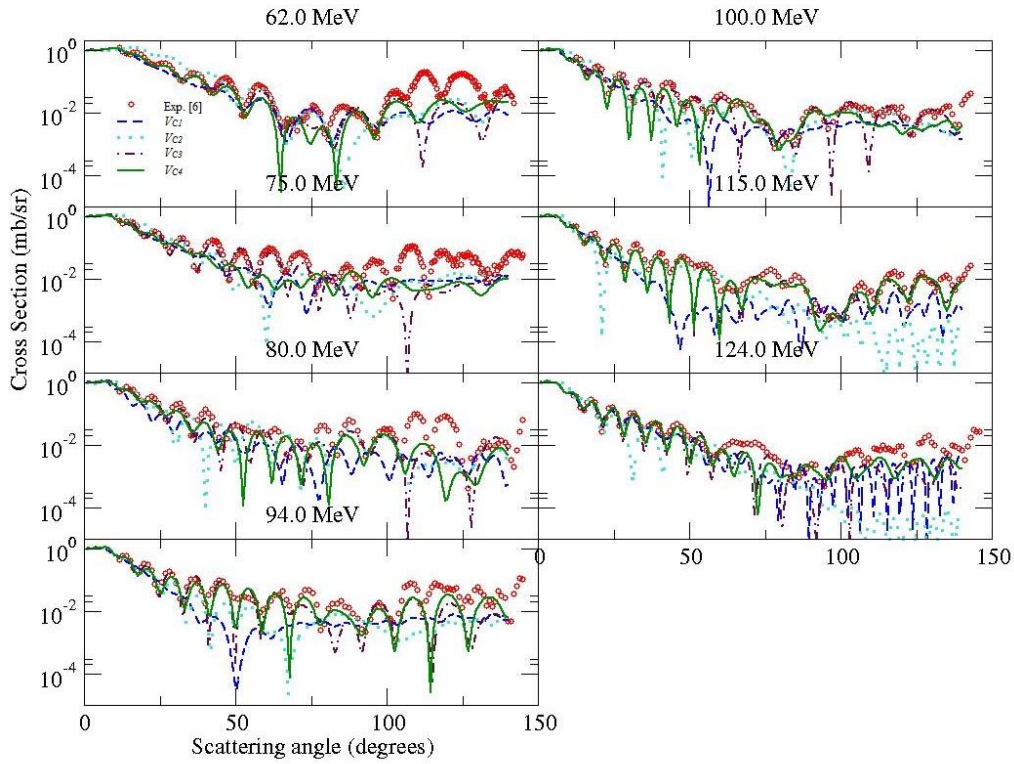


Figure 3. Comparison of the experimental and calculated angular distributions for the $^{16}\text{O}+^{12}\text{C}$ elastic scattering at $E_{LAB}=62, 75, 80, 94.8, 100, 115.9$ and 124 MeV (x -axis characterizes the scattering angles in the CM frame and the y -axis corresponds to the Rutherford differential cross sections in logarithmic scale). The available experimental data are given by red circles. The fits, obtained from four different phenomenological potential sets with the related parameters given in Table 1, are represented by the lines (dashed blue line used for V_{C1} type potential, the solid light blue line for V_{C2} type potential, solid purple line for V_{C3} type potential and dashed-dotted green line for V_{C4} type potential).

4. Conclusion and Comment

The conventional OM calculations of the $^{16}\text{O}+^{12}\text{C}$ elastic scattering with 6- or 9-parameter optical potentials for various energies have been studied by many authors, but a systematic analysis including the evaluation of all the possible phenomenological Woods-Saxon type nuclear potential sets has not been simultaneously given before. In this study, we have presented comparative differential cross-section analyses for the elastic scattering of $^{16}\text{O}+^{12}\text{C}$ system by considering different nuclear potential sets in standard OM formalism. The angular distribution data on $^{16}\text{O}+^{12}\text{C}$ scattering have been reproduced for the bombarding energies $E_{LAB}=62, 75, 80, 94.8, 100, 115.9$ and 124 MeV by using $\text{WS2}+i(\text{WS})$, $\text{WS2}+i(\text{WS2})$, $\text{WS2}+i(\text{WS}+\text{WSD})$ and $\text{WS2}+i(\text{WS2}+\text{WSD})$ type phenomenological potentials with free parameters. The agreement between the measured data and the outcomes of the proposed potential sets has been evaluated by χ^2 calculations. Within the limitations of this study, it can be concluded that the latter potentials (V_{C3} and V_{C4}), which contain imaginary surface terms, have described the experimental data more successfully than the ones consisting of a pure volume term only. It was shown that, similar results could be produced by using V_{C3} and V_{C4} type potential sets. Furthermore, one-channel OM analyses of V_{C4} type central potential shape have been also introduced for the first time with this work for 62 and 75 MeV data.

Acknowledgment

This study is a part of M.Sci. Thesis of G. Cof, submitted to the University of Süleyman Demirel, Graduate School of Natural and Applied Sciences, Turkey.

References

- [1] M.E. Brandan and G.R. Satchler, "The interaction between light heavy-ions and what it tells us," *Phys. Rep.*, 285 (4-5), 143-243, 1997.
- [2] G.R. Satchler, *Introduction to Nuclear Reactions*, Palgrave Macmillan UK, London, 1990.
- [3] G.R. Satchler, *Direct Nuclear Reactions*, Oxford University Press, New York, 1983.
- [4] P.E. Hodgson, *The Nucleon Optical Model*, World Scientific Publishing Co. Pte. Ltd., London, 1994.
- [5] I. Boztosun, "Systematic investigation of light heavy-ion reactions" *Phys. Atom. Nucl.*, 65 (4), 607-611, 2002.
- [6] M.P. Nicoli, F. Haas, R.M. Freeman, S. Szilner, Z. Basrak, A. Morsad, G. R. Satchler, and M.E. Brandan, "Detailed study and mean field interpretation of $^{16}\text{O}+^{12}\text{C}$ elastic scattering at seven medium energies" *Phys. Rev. C*, 61, 034609, 2000.
- [7] S. Szilner, M.P. Nicoli, Z. Basrak, R.M. Freeman, F. Haas, A. Morsad, M.E. Brandan, and G.R. Satchler, "Refractive elastic scattering of carbon and oxygen nuclei: The mean field analysis and Airy structures," *Phys. Rev. C*, 64, 064614, 2001.
- [8] M.E. Kürkçüoğlu and H. Aytekin, "An Investigation of the $^{16}\text{O}+^{16}\text{O}$ elastic scattering by phenomenological and double-folding potentials in optical model formalism at the energies between $E_{\text{LAB}}=75$ and 145MeV," *Indian J. Phys.*, 80 (6), 641-645 2006.
- [9] M.P. Nicoli, F. Haas, R.M. Freeman, N. Aissaoui, C. Beck, A. Elanique, R. Nouicer, A. Morsad, S. Szilner, Z. Basrak, M.E. Brandan, and G.R. Satchler, "Elastic scattering of $^{16}\text{O}+^{16}\text{O}$ at energies E/A between 5 and 8 MeV," *Phys. Rev. C*, 60, 064608, 1999.
- [10] A.A. Ogloblin, Yu.A. Glukhov, W.H. Trzaska, A.S. Dem'yanova, S.A. Goncharov, R. Julin, S.V. Klebnikov, M. Mütterer, M.V. Rozhkov, V.P. Rudakov, G.P. Tiorin, D.T. Khoa, and G.R. Satchler, "New measurement of the refractive, elastic $^{16}\text{O}+^{12}\text{C}$ scattering at 132, 170, 200, 230, and 260 MeV incident energies," *Phys. Rev. C*, 62, 044601, 2000.
- [11] M.E. Kürkçüoğlu, H. Aytekin, and I. Boztosun, "Optical model analysis of the $^{16}\text{O}+^{16}\text{O}$ nuclear scattering reaction around $E_{\text{LAB}}=5\text{MeV/nucleon}$," *G. U. Journal of Science* 19 (2), 105-112, 2006.
- [12] Sh Hamada, N. Burtebayev, K.A. Gridnev, and N. Amangeldi, "Further investigation of the elastic scattering of ^{16}O , ^{14}N and ^{12}C on the nucleus of ^{27}Al at low energies," *Phys. Scr.* 84 (4), 045201, 2011.
- [13] A.T. Rudchik, Yu.O. Shyrma, K.W. Kemper, K. Rusek, E.I. Koshchy, S. Kliczewski, B.G. Novatsky, O.A. Ponkratenko, E. Piasecki, G.P. Romanyshyna, Yu.M. Stepanenko, I. Strojek, S.B. Sakuta, A. Budzanowski, L. Głowacka, I. Skwirczyńska, R. Siudak, J. Choiński, and A. Szczurek, "Elastic and inelastic scattering of $^{14}\text{C}+^{18}\text{O}$ versus $^{12,13}\text{C}+^{18}\text{O}$ and $^{14}\text{C}+^{16}\text{O}$," *Eur. Phys. J. A* 47, 50, 2011.
- [14] A.T. Rudchik, Yu.O. Shyrma, K.W. Kemper, K. Rusek, E.I. Koshchy, S. Kliczewski, B.G. Novatsky, O.A. Ponkratenko, E. Piasecki, G.P. Romanyshyna, Yu.M. Stepanenko, I. Strojek, S.B. Sakuta, A. Budzanowski, L. Głowacka, I. Skwirczyńska, R. Siudak, J. Choiński, and A. Szczurek, "Elastic and inelastic scattering of $^{13}\text{C}+^{18}\text{O}$ versus $^{12}\text{C}+^{18}\text{O}$ and $^{13}\text{C}+^{16}\text{O}$," *Nucl. Phys. A* 852 (1), 1-14, 2011.
- [15] Sh Hamada, N. Burtebayev, N. Amangeldi, K.A. Gridnev, K. Rusek, Z. Kerimkulov, and N. Maltsev, "Phenomenological and semi-microscopic analysis for ^{16}O and ^{12}C elastically scattering on the nucleus of ^{16}O and ^{12}C at energies near the Coulomb barrier," *J. Phys. Conf. Ser.* 381 (1), 012130, 2012.
- [16] D.T. Khoa, W.V. Oertzen, H.G. Bohlen, and F. Nuoffer, "Study of diffractive and refractive structure in the elastic $^{16}\text{O}+^{16}\text{O}$ scattering at incident energies ranging from 124 to 1120 MeV," *Nucl. Phys. A* 672 (1-4), 387-416, 2000.
- [17] M.E. Brandan, A. Menchaca-Rocha, L. Trache, H.L. Clark, A. Azhari, C.A. Gagliardi, Y.-W. Lui, R.E. Tribble, R.L. Varner, J.R. Beene, and G.R. Satchler, "Refractive elastic scattering of ^{16}O by ^{12}C at 300 MeV," *Nucl. Phys. A*, 688 (3-4), 659-668, 2001.
- [18] A.A. Ogloblin, D.T. Khoa, Y. Kondo, Yu.A. Glukhov, A.S. Dem'yanova, M.V. Rozhkov, G.R. Satchler, and S.A. Goncharov, "Pronounced Airy structure in elastic $^{16}\text{O}+^{12}\text{C}$ scattering at $E_{\text{lab}}=132\text{MeV}$," *Phys. Rev. C* 57, 1797, 1998.
- [19] M.E. Kürkçüoğlu, H. Aytekin, and I. Boztosun, "An investigation of the $^{16}\text{O}+^{16}\text{O}$ elastic scattering by using alpha-alpha double folding potential in optical model formalism," *Mod. Phys. Lett. A* 21 (29), 2217-2232, 2006.

- [20] A.H. Al-Ghamdi, A.A. Ibraheem, and M. El-Azab Farid, "An investigation of $^4\text{He}+^{12}\text{C}$ and $^4\text{He}+^{16}\text{O}$ reactions using the cluster model," *Commun. Theor. Phys.* 58 (1), 135-140 (2012).
- [21] V.Yu. Denisov and O.I. Davidovskaya, "Elastic scattering of heavy nuclei and nucleus-nucleus potential with repulsive core" *Phys. Atom. Nucl.* 73 (3), 404-411, 2010.
- [22] Y.X. Yang and Q.R. Li, "Elastic $^{16}\text{O}+^{20}\text{Ne}$ scattering from a folding model analysis," *Phys. Rev. C* 84, 014602, 2011.
- [23] A. Barioni, J.C. Zamora, V. Guimarães, B. Paes, J. Lubian, E.F. Aguilera, J.J. Kolata, A.L. Roberts, F.D. Becchetti, A. Villano, M. Ojaruega, and H. Jiang, "Elastic scattering and total reaction cross sections for the ^8B , ^7Be , and $^6\text{Li}+^{12}\text{C}$ systems," *Phys. Rev. C* 84, 014603, 2011.
- [24] M.E. Kürkcüoğlu, G. Cof, H. Aytekin, and I. Boztosun, "Introducing a global optical model approach for analysing $^{16}\text{O}+^{16}\text{O}$ elastic scattering at 5-10MeV/nucleon region," *SDU Journal of Science (e-journal)* 8 (1), 71-86 (2013).
- [25] M.A. Hassanain, "Cluster folding and coupled-channels analysis of $^{16}\text{O}+^{16}\text{O}$ elastic and inelastic scattering," *Brazilian J. of Phys.* 44 (6), 895 (2014).
- [26] A.S. Demyanova, H.G. Bohlen, A.N. Danilov, S.A. Goncharov, S.V. Khlebnikov, V.A. Maslov, Yu.E. Penionzkevich, Yu.G. Sobolev, W. Trzaska, G.P. Tyurin, and A.A. Ogloblin, " $^{12}\text{C}+^{12}\text{C}$ large angle elastic scattering at 240 MeV," *Nucl. Phys. A* 834 (1-4), 473c-475c, 2010.
- [27] Y. Küçük and I. Boztosun, "Global examination of the $^{12}\text{C}+^{12}\text{C}$ reaction data at low and intermediate energies," *Nucl. Phys. A* 764, 160-180, 2006.
- [28] D.T. Khoa, N.H. Phuc, D.T. Loan, and B.M. Loc, "Nuclear mean field and double-folding model of the nucleus-nucleus optical potential," *Phys. Rev. C* 94, 034612 2016.
- [29] M.A. Hassanain, "Investigation of $^{16}\text{O}+^{12}\text{C}$ refractive elastic scattering using the α -cluster model potential," *Eur. Phys. J. A* 52, 8, 2016.
- [30] S. Ohkubo, Y. Hirabayashi, and A.A. Ogloblin, "Existence of inelastic supernumerary nuclear rainbow in $^{16}\text{O}+^{12}\text{C}$ scattering," *Phys. Rev. C* 96, 024607, 2017.
- [31] S. Hossain, M.N.A. Abdullah, K.M. Hasan, M. Asaduzzaman, M.A.R. Akanda, S.K. Dasa, A.S.B. Tariq, M.A. Uddin, A.K. Basak, S. Ali, and F.B. Malik, "Shallow folding potential for $^{16}\text{O}+^{12}\text{C}$ elastic scattering," *Phys. Lett. B* 636, 248, 2006.
- [32] Sh. Hamada, I. Bondok, and M. Abdelmoatmed, "Double folding potential of different interaction models for $^{16}\text{O}+^{12}\text{C}$ elastic scattering," *Brazilian J. of Phys.* 44 (6), 740-745, 2016.
- [33] A.T. Rudchik, Yu.O. Shyrma, K.W. Kemper, K. Rusek, E.I. Koshchy, S. Kliczewski, B.G. Novatsky, O.A. Ponkratenko, E. Piasecki, G.P. Romanyshyna, Yu.M. Stepanenko, I. Strojek, S.B. Sakuta, A. Budzanowski, L. Głowacka, I. Skwirczyńska, R. Siudak, J. Choiński, and A. Szczurek, "Isotopic effects in elastic and inelastic $^{12}\text{C}+^{16,18}\text{O}$ scattering," *Eur. Phys. J. A* 44 (2), 221-231, 2010.
- [34] I. Boztosun, O. Bayrak, and Y. Dagdemir, "Comparative study of the $^{12}\text{C}+^{24}\text{Mg}$ system with deep and shallow potentials," *Int. J. Mod. Phys. E* 14 (4), 663-673, 2005.
- [35] I. Boztosun, Y. Dagdemir, and O. Bayrak, "The examination of the $^{12}\text{C}+^{24}\text{Mg}$ elastic scattering around the Coulomb barrier," *Phys. Atom. Nucl.* 68 (7), 1153-1159, 2005.
- [36] K.A. Gridnev, E.E. Rodionova, and S.N. Fadeev, "Description of elastic scattering in the $^{16}\text{O}+^{16}\text{O}$ and $^{16}\text{O}+^{12}\text{C}$ systems," *Phys. Atom. Nucl.* 71 (7), 1262-1266, 2008.
- [37] H. Feshbach, C.E. Porter and V.F. Weisskopf, "Model for nuclear reactions with neutrons," *Phys. Rev.* 96 (2), 448, 1954.
- [38] R.D. Woods and D.S. Saxon, "Diffuse surface optical model for nucleon-nuclei scattering," *Phys. Rev.* 95 (2), 577, 1954.
- [39] I.J. Thomson, "Coupled reaction channels calculations in nuclear physics," *Comput. Phys. Rep.* 7, 167-212, 1988.